



Heteropolar Bonding and a Position-Space Representation of the 8 – N Rule

Journal:	<i>Dalton Transactions</i>
Manuscript ID	DT-FRO-10-2015-004140.R1
Article Type:	Frontier
Date Submitted by the Author:	02-Dec-2015
Complete List of Authors:	Wagner, Frank; MPI CPfS, Chemical Metals Science Bende, David; MPI CPfS, Chemical Metals Science Grin, Yuri; MPI CPfS, Chemical Metals Science



Journal Name

ARTICLE

Heteropolar Bonding and a Position-Space Representation of the 8 – *N* Rule

F. R. Wagner,^a D. Bende,^a Yu. Grin^aReceived 00th January 20xx,
Accepted 00th January 20xx

DOI: 10.1039/x0xx00000x

www.rsc.org/

Chemical bonding models are one of the most powerful tools in chemistry and provide essential guidance in the understanding of composition and structure of chemical compounds, as well as in the development of new preparation routes. Facing the tremendous diversity of crystal structures and properties of intermetallic compounds, it is highly desirable to make the predictive power of chemical bonding models also available for this field of inorganic chemistry. Within the framework of quantum-chemical position-space analysis the concept of the 8–*N* rule is recovered and extended for a consistent and quantitative treatment of heteropolar bonding situations as in compounds of the MgAgAs type and their relatives. A first evaluation of the predictive capabilities of the position-space view is obtained in the analysis of 51 zinc-blende, wurtzite and rock-salt-type compounds. An outlook on future investigations is given and modifications of main-group elements and (pseudo) main-group compound families are classified within the presented model framework.

1. Introduction

In the chemistry of intermetallic compounds only a few chemical bonding models are established.^[1,2] The main reason for that is the general demand on valence electrons. Despite the relatively short interatomic distances in the crystal structures being often comparable or smaller than a sum of the respective atomic or even covalent radii, these interactions cannot be interpreted as 2-center-2-electron bonds due to the lack of electrons in the system. For compounds of elements from the groups 14 to 17 with a sufficient number of electrons in the systems, the crystal structures are rationalized according to the 8–*N* rule, where *N* is the number of valence electrons.^[3,4] The number of 8–*N* nearest neighbours is equal to the number of 2-electron-2-center bonds. The Zintl-Klemm concept recovers the 8–*N* rule for homopolar^[5,6] and heteropolar^[7] bonding situations in polyanionic substructures. In NaIn, for example, a cationic and an anionic partial structure coexist after the formal charge transfer as Na⁺In[−]. The electronic configuration of In[−] allows a diamond-like homoatomic indium-partial structure with four 2-electron-2-center bonds per anion. In this framework the interaction between the resulting polyanionic covalent network and the Na⁺ cations is purely ionic. If the valence electron count per anion exceeds 8, the generalized 8–*N* rule may be applied.^[8,9] The excess electrons above 8 remain on the electropositive atoms either for the formation of bonds within a polycation or as lone pairs.^[10] In case of multi-component compounds, an explicit account of heteropolar bonding within the anionic

partial structure is circumvented by treating heteroanions as a whole thus avoiding specification of atomic species.^[7]

For the reduced number of valence electrons compared to the Zintl-like bonding situation, the Wade-Mingos rules define the number of valence electrons required for the stabilization of the anionic partial structures, e.g., in cluster compounds like CaB₆.^[11,12] The bonds between the clusters remain 2-center-2-electron ones. Within the cluster, multi-center bonding, in particular 3-center bonding, accounts for electron demand.

A further decrease of the valence electron concentration leads to the formation of multi-center bonding with more than three centers per bond like in brass phases. Within the Hume-Rothery mechanism, a decreasing valence electron concentration, e.g. from CuZn₃ to CuZn, allows for a smaller and smaller Brillouin zone to accommodate the valence electrons and is therefore accompanied by a structural change at a critical value.^[13–15]

A recent contribution reports the extension of the 8–*N* rule to intermetallic compounds with heteropolar bonding.^[16] In this work the model's predictive capabilities are considered as an outlook on future research. Finally, different families of intermetallic compounds are classified within the conceptual framework presented.

2. The 8–*N* rule from a formal perspective

The 8–*N* rule for solid compounds can be applied in two different ways. Within the first view the formal charges are

^a Max-Planck-Institut für Chemische Physik fester Stoffe, Nöthnitzer Straße 40, 01187 Dresden, Germany.

assigned according to the electronegativity differences and assuming complete transfer of valence electrons from the more electropositive component to the more electronegative one (Figure 1 left). The number of homoatomic bonds is then given as $8-N$ with N being the number of valence electrons of the anion after the formal charge transfer. For InSb this yields $8 - 8 = 0$ bonds. For GaSe with 9 valence electrons, the same procedure leads to maximally possible transfer of 2 electrons from Ga to Se, i. e. Ga^{2+} and Se^{2-} species. The generalized $8-N$ rule in this case predicts one Ga–Ga bond and no Se–Se bonds.

The second view emphasizes the heteroatomic connections. For example in InSb, the heteroatomic bonding pattern of four-bonded (4b)In and four-bonded (4b)Sb, is presumed from the nearest neighbour coordination spheres, i.e. tetrahedral In@Sb_4 and tetrahedral Sb@In_4 (Figure 1 right). The formal charges are calculated assuming that one half of each bond (1 electron per bond) is assigned to an atom.^[4] The so-obtained formal charges in InSb, In^{1-} and Sb^{1+} , conflict the expectation from the electronegativity difference. In this picture both components (4b)In¹⁻ and (4b)Sb¹⁺ have a formal octet configuration and InSb is identified as a valence compound with tetrahedral In–Sb bonding. Likewise for GaSe, a network of tetrahedral Ga@GaSe_3 and pseudo-tetrahedral $|\text{Se@Ga}_3$ units is detected which yields formal charges Ga^{1-} and Se^{1+} , again in conflict with electronegativity difference.

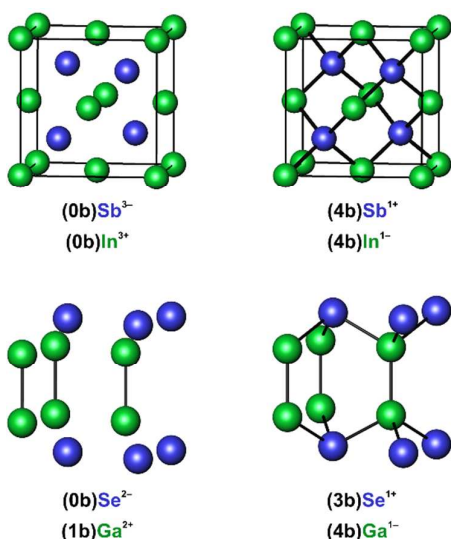


Fig. 1 Homopolar (left) and heteropolar (right) structure pattern in InSb (top) and $[\text{Ga}_2]\text{Se}_2$ (bottom) as obtained from the $8-N$ rule.

The two complementary ways of working with the $8-N$ rule highlight different structural aspects of InSb and GaSe, although both are based on the generalized $8-N$ rule. The difference originates from an inconsistent treatment of the heteropolar bonds. In the first approach they are ignored, treated ‘on-top’ of the $8-N$ rule and the anion’s valence electrons are counted as 1-center-2-electron lone pairs (Figure 1 left). In the second protocol, the nearest-neighbour diagram is *de facto* used to define heteropolar bonds, and they are counted like non-polar covalent 2-center-2-electron bonds

resulting in formal charges which conflict with the electronegativity differences (Figure 1 right). The approach we propose for a consistent and quantitative treatment of heteropolar bonding, leads to the unification of the effective QTAIM charges and the formal charges of pseudo-atomic species.

3. Covalent bonds, lone pairs and heteropolar bonds

According to the Lewis model, a homopolar bond is characterized by an equal electronic contribution of the bonded atoms (Figure 2 left).^[16] The formation of lone pairs represents the opposite case to homopolar bonding (Figure 2 right). The lone pair completely belongs to one atom displaying ultimate polar character of the valence region. This situation is characteristic for ionic compounds like NaCl or noble-gas crystals with van-der-Waals interactions.

In a heteropolar bond the bonded atoms contribute different electron numbers to the bond region (Figure 2 middle). Analogous to a homopolar bond, the non-polar part of each bonded atom has the same value. It is determined by the contribution of the minority participating species L .^[17] The remaining electrons of the bond region belong to the majority contributing species and constitute the polar part of the heteropolar bond. The non-polar contribution may be termed as the covalent part of the heteropolar bond. The polar contribution is made by one atom only, i. e., is of 1-center type and may therefore be termed the ‘hidden lone-pair’ part of the heteropolar bond. This way, the heteropolar bond is interpreted as a superposition of polar and non-polar parts within the same valence region. In Fig. 2 the ‘decomposition’ of the bond region B^X (orange and teal coloured mini-squares) is made only to illustrate the electronic contributions. There is no real spatial separation within one atomic region between electrons of the polar and non-polar parts, respectively. Although this scheme is primarily intended to prepare for the subsequent position space treatment^[16] it should be understood as an even more general approach including also cases of overlapping atomic regions.

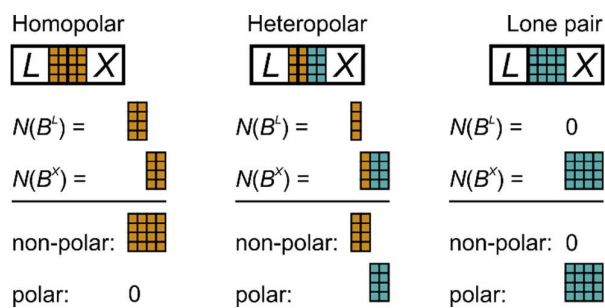


Fig. 2 Homopolar bonds, heteropolar bonds and lone pairs: the bold black lines represent the atomic boundaries of X and L atoms; the orange-teal coloured part represents the bond region B with the total electronic population always symbolized by 16 mini-squares. $N(B^L)$ and $N(B^X)$ are the electron contributions of atoms L and X , respectively, to the bond region B . The orange mini-squares symbolize the non-polar part; the teal mini-squares symbolize the polar part of the bond.

4. The 8–*N* rule from a position-space perspective

4.1 Heteropolar bonds in position space

The formal treatment of heteropolar bonding suggested above requires a well-defined measure of bond polarity in order to assign the polar and non-polar parts for a given bonding situation. For the purpose of a quantum-chemical realization of the proposed procedure, a position-space perspective was chosen, which closely mimics the formal procedure described above.

The assignment of atomic regions is effectuated in the framework of the QTAIM (quantum theory of atoms in molecules) method, which uses the electron density as central quantity.^[18] Topological analysis of the electron density yields local maxima at the atomic positions and individual atomic regions containing the atomic nucleus and being bounded by surfaces of zero-flux in density gradient. This way an exhaustive partitioning of position space in non-overlapping atomic regions is obtained. Integration of the electron density within the atomic region of atom *X* yields its electronic population $\bar{N}(X)$ and effective atomic charge

$$Q^{\text{eff}}(X) = Z(X) - \bar{N}(X) \quad (1)$$

As an additional ingredient another partitioning of position space is needed which should separate atomic core regions from valence regions and split the valence region into bonds and lone pair parts. This is achieved with the aid of the topological analysis of the ELI-D (electron localizability indicator) distribution.^[19] Within a nutshell, the ELI-D distribution in position space locally depicts the charge needed to form a fixed fraction of a same-spin electron pair. It provides a measure of the extent an electron is alone, i.e. localized, at a certain point in space. ELI-D represents one possible generalization of the electron localisation function (ELF)^[20a] originally defined in the closed-shell Hartree-Fock framework^[20b] for the correlated, open-shell, time-dependent case. Zero-flux surfaces of the ELI-D basin regions divide the whole space into onion shell-like atomic core regions C^X and valence regions *B* according to the Aufbau principle.^[21,22] Integration of the electron density within the ELI-D regions obtained yields their electronic populations.

The evaluation of bond polarities is achieved in a final step called the ELI-D/QTAIM intersection technique, where the ELI-D and electron density are superimposed to evaluate the QTAIM atomic contributions to the ELI-D valence regions *B* (Figure 3). For this purpose, the electron density within the ELI-D regions B^X is integrated to $\bar{N}(B^X)$. The ratio between $\bar{N}(B^X)$ and the complete electron population of the valence region $\bar{N}(B)$ gives the polarity as bond fraction $p(B^X)$ with *X* being the majority contributing species (similar to the Raub-Jansen index).^[23]

$$p(B^X) = \frac{\bar{N}(B^X)}{\bar{N}(B)} \quad (2)$$

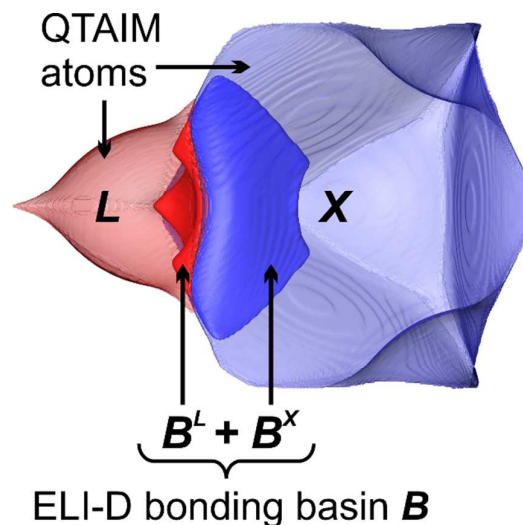
In a non-polar bond both QTAIM atoms contribute half of the electrons of the common bond region *B*, $p(B^X) = 0.5$. A lone-pair like valence region is characterized by $p(B^X) = 1.0$. Heteropolar bonding is indicated by bond fractions between 0.5 and 1.0.

In order to calculate the covalent character of an ELI-D valence basin $cc(B)$ according to the suggested formal scheme (Figure 2), the following equation applies:

$$cc(B) = 2 \cdot [1 - p(B^X)] \quad (3)$$

For a non-polar covalent bond with $p(B^X) = 0.5$, $cc(B) = 1$; for a lone-pair like ELI-D valence region with $p(B^X) = 1$, $cc(B) = 0$.

Fig. 3 The ELI-D/QTAIM intersection technique. Transparent light red



and blue regions are QTAIM atoms *L* and *X*; the ELI-D bonding region *B* is intersected by the QTAIM atoms which yields two separate regions B^L (dark red) and B^X (dark blue).

4.2 Electron counting in position space

Position-space topological analysis of the electron density and ELI-D allows a consistent and quantitative treatment of heteropolar bonding. Also the concept of the 8–*N* rule can be recovered in position space as is shown in the following. The ‘eight’ in ‘8–*N*’ counts the number of valence electrons around an atom in a Lewis diagram no matter if they are contained in a formal covalent bond or a lone pair. The same formalism is applied in position space by counting all electrons in ELI-D valence regions around a particular ELI-D core region of an atom *X*. The ELI-D valence regions *B*, which share a surface with the ELI-D core region C^X form the access electron set s_X , and the sum of the corresponding electron populations is the ELI-D access electron number $\bar{N}_{\text{acc}}^{\text{ELI}}(C^X)$.

$$\bar{N}_{\text{acc}}^{\text{ELI}}(C^X) = \sum_{i=1}^{s_X} \bar{N}(B_i) \quad (4)$$

The ‘*N*’ in ‘8–*N*’ counts the number of valence electrons owned by a particular atom in a Lewis diagram. The corresponding position-space valence-electron number is calculated as the difference between the electron population of a particular QTAIM atom and the corresponding ELI-D core-region population.

$$\bar{N}_{\text{val}}^{\text{ELI}}(X) = \bar{N}(X) - \bar{N}(C^X) \approx \sum_{i=1}^{s_X} \bar{N}(B_i^X) \quad (5)$$

It is also given by summation over $\bar{N}(B_i^X)$, the QTAIM atom’s contributions to the ELI-D valence regions within its access electron set.⁵ The position-space representation of the 8–*N* rule is then:

$$N_{\text{cb}}^{\text{ELI}}(X) = \bar{N}_{\text{acc}}^{\text{ELI}}(C^X) - \bar{N}_{\text{val}}^{\text{ELI}}(X), \quad (6)$$

where $N_{cb}^{ELI}(X)$ gives the effective number of covalent bonds. The access electron number $\bar{N}_{acc}^{ELI}(C^X)$ represents the 'eight', the valence electron number $\bar{N}_{val}^{ELI}(X)$ represents the 'N' in '8-N'.

In the formalism presented there is a direct connection between the 8-N rule and the covalent character cc of an ELI-D valence basin:

$$N_{cb}^{ELI}(X) = \bar{N}_{acc}^{ELI}(C^X) - \bar{N}_{val}^{ELI}(X) \approx \sum_{i=1}^{s_x} \bar{N}(B_i) - \sum_{i=1}^{s_x} \bar{N}(B_i^X)$$

$$= \sum_{i=1}^{s_x} [\bar{N}(B_i) - p(B_i^X) \cdot \bar{N}(B_i)] = \frac{1}{2} \sum_{i=1}^{s_x} [2 - 2p(B_i^X)] \cdot \bar{N}(B_i)$$

$$= \frac{1}{2} \sum_{i=1}^{s_x} cc(B_i) \cdot \bar{N}(B_i) \quad (7)$$

The covalent character represents the interpretation of heteropolar bonding (Fig. 2) in the ELI-D/QTAIM framework.

5. Position-space 8-N rule for main-group compounds

The position-space representation of the 8-N rule including a consistent and quantitative treatment of heteropolar bonding is applied to a number of main-group intermetallic compounds (Figure 4). Computational details are given in the reference.^[16] The analysed phases are main-group MgAgAs-type (half-Heusler) compounds LiInSn, LiInGe, LiAlSi, LiAlGe, BeAlB, LiMgPn (Pn=N-Bi), Zintl phases LiSi, NaP, Na₂S₂, zinc-blende-type InSb, GaAs, AlP, BN, BeS, and fluorite-type compounds Mg₂Si, Li₂S. The black line and crosses in Figure 4 represent the formal 8-N rule with respect to the underlined anion. For example, Si¹⁻ in LiSi has formally 5 valence electrons and 3 non-polar Si-Si bonds per Si. The position-space results (orange crosses) are always close to the formal picture indicating that the investigated compounds are octet compounds with $\bar{N}_{acc}^{ELI}(C^E) = 8 \pm 0.3$ in most cases.⁵⁹ This is characteristic for a bonding pattern in agreement with the position-space 8-N rule. Accordingly, the compounds analysed show between 2.95 (LiSi) and 0.24 (Li₂S) covalent bonds per anion.

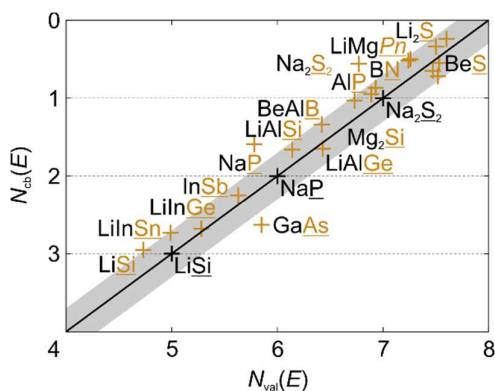


Fig. 4 Position space 8-N rule for main-group compounds. The black line and crosses represent the formal 8-N rule. The underlined element is the anion E . Orange crosses represent the position-space view. The grey shadow indicates the region $\bar{N}_{acc}^{ELI}(C^E) = 8 \pm 0.3$.

Compared to the formal 8-N rule, the position-space view allows a consistent and quantitative treatment of compounds with heteropolar bonding (zinc-blende, MgAgAs type) and non-tetrahedral coordination (fluorite, MgAgAs type). It is also possible to identify non-octet compounds e.g. Mg (hcp): $\bar{N}_{acc}^{ELI}(C^{Mg}) = 3.8$.

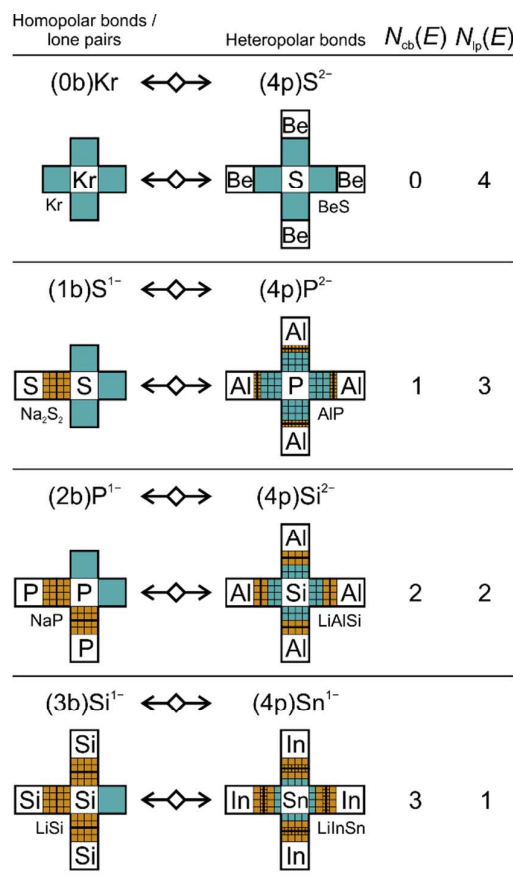


Fig. 5 Position-space representation of the 8-N rule: conceptual analogy between the bonding patterns of compounds with homopolar bonding/lone pairs (0b–3b, left) and compounds with heteropolar bonding (4p, right). Only the valence region of the central atom is shown completely. The anions' number of covalent bonds $N_{cb}(E)$, the anions' number of lone pairs $N_{lp}(E)$ and the QTAIM or formal charges (cf. Text) displayed in the superscripts of the elemental symbols are rounded to integers for illustration. The double-arrow symbol indicates the described analogy between the compounds with (0b–3b) E and (4p) E bonding patterns.

The equal treatment of compounds with exclusively homopolar bonding/lone pairs and compounds with exclusively heteropolar bonds leads to an important analogy between the bonding patterns (Figure 5): according to the 8-N rule, a component with 4, 5, 6, 7, or 8 valence electrons realizes the respective bonding patterns (4b), (3b, 1p), (2b, 2p), (1b, 3p), and (4p), where symbol nb denotes n two-center–two-electron non-polar bonds and symbol mlp m two-electron lone pairs (Figure 5 left panel). The compounds with exclusive heteropolar bonding (e.g. zinc-blende, MgAgAs type) realize the bonding pattern (4p) with four equal heteropolar bonds, which are interpreted as a mixture of a partial non-polar (covalent) part b' and a polar (hidden lone-pair) part lp' , i.e.

$$(4p) = (4xb', 4[1-x]lp') \quad (8)$$

where x indicates the bond polarity (ranging between $x = 1$ for the non-polar covalent bond and $x = 0$ for the fully polar lone-pair like case).

The case of zero covalent bonds and four lone pairs per atom occurs for the noble gas Kr (4lp) and roughly for sulphur in the ionic zinc-blende-type compound BeS (4p with $x = 0.09$). One covalent bond and three lone pairs occur for sulphur in $\text{Na}_2[\text{S}_2]$ (1b, 3lp). An equivalent of one covalent bond and three lone pairs is mixed in four heteropolar bonds in AlP (4p with $x = 0.24$). Accordingly, the remaining compounds in Figure 5 illustrate the correspondence between bonding situations with homopolar bonding/lone pairs and heteropolar bonding for the cases with two and three (effective) covalent bonds per anion.

The consistent and quantitative treatment of heteropolar bonding proposed here unites the two views on the $8-N$ rule in solid state chemistry (Figure 1). It leads to a unification of the effective and the formal charge of the pseudo-atomic species. The starting point for InSb is the formal view as 4-bonded Sb leading to $(4\text{b})\text{Sb}^{1+}$ with the positive formal charge 1+ for Sb. Using 1.99 electrons in each of the four surrounding Sb-In bond basins in the ELI-D representation⁵⁶ instead of the formal two yields $(3.98\text{b})\text{Sb}^{1.02+}$. Introduction of bond polarity with the aid of ELI-D/QTAIM basin intersection yields a covalent (non-polar) character of $cc = 0.58$ and a hidden-lone-pair (polar) character of 0.42 leads to $(2.32\text{b}', 1.66\text{lp}')\text{Sb}^{0.64-}$. Thus the formal charge of 0.64- is calculated analogously to Ref. [4] as $5 - 2.32 - 2 \times 1.66$ (assuming that one half of each bond and the full lone pair is assigned to an atom). Taking into account the 0.19 electron underpopulation of the Sb core^[22] (45.81 electrons instead of 46) and the corresponding overpopulation of the ELI-D valence region, the so-corrected formal charge is 0.45-, which is within rounding error identical to the obtained QTAIM effective charge of -0.46.

For GaSe the number of valence electrons per formula unit of 9.49 given by ELI-D/QTAIM already indicates the polycationic character of the compound⁵⁶. Each Se atom with an effective QTAIM charge of -0.69 displays three heteropolar Se-Ga bonds each with a population of 1.79 electrons and one lone pair with a population of 2.85 electrons. Neglecting bond polarity it would be formulated as $(3\text{b}, 1\text{lp})\text{Se}^{1+}$, while taking polarity into account changes the charge assignment to $(3\text{p}, 1\text{lp})\text{Se}^{2-}$. The ELI-D basin populations results in $(2.69\text{p}, 1.43\text{lp})\text{Se}^{2-}$. The ELI-D/QTAIM basin intersection yields a covalent character of 0.49 and a hidden lone pair character of 0.51 for each bonding basin, which finally yields $(1.32\text{b}', 1.37\text{lp}'; 1.43\text{lp})\text{Se}^{0.92-}$, where b' and lp' are partial non-polar (covalent) part a polar (hidden lone-pair) part, respectively, and lp is the number of real two-electron lone pairs:

$$(\text{yp}; [4-y]\text{lp}) = (y[x]\text{b}', y[1-x]\text{lp}'; [4-y]\text{lp}) \quad (9)$$

The formal charge of 0.92- is calculated in this case as $6 - 1.32 - 2 \times 1.37 - 2 \times 1.43$. The connection with the QTAIM effective charge needs to take into account the ELI-D core underpopulation^[22] of 0.22 electrons (27.78 electrons core population for Se) and the corresponding valence shell overpopulation. This correction finally yields $(1.32\text{b}', 1.37\text{lp}'; 1.43\text{lp})\text{Se}^{0.70-}$, which displays that the Se formal charge of 0.70- is within a rounding error identical to the QTAIM effective charge of -0.69 given above.

5. Perspective on predictive capabilities

Binary 1:1 compounds with eight valence electrons and the elemental structures of tetrels were investigated. The compounds are solely comprised of main-group elements within the Li-Rb-I-F

rectangle of the periodic table which gives 51 different compounds (BSb is experimentally not known). Such binary compounds AE crystallize either with the rock-salt, zinc-blende, wurtzite or graphite type. h -BN shows a ordered substitution variant of the graphite type. To identify the most stable structure type, each compound was optimized in the DFT/PBE framework.[‡] The optimized structures agree with the experimentally observed ones. GaN is found to be more stable in the zinc-blende type^[24] than in the wurtzite type.^[25] For LiCl, LiBr and LiI the wurtzite type was found to be more stable than the rock-salt type. This is in accordance with previous calculations^[26] and the recent synthesis of wurtzite modifications of LiCl^[27], LiBr and LiI.^[28]

The ELI-D topologies^{††} of the investigated compounds show attractors on the direct connection lines between the nearest neighbours in the structure, i.e. three equivalent attractors per atom in the graphite-like structures, four in the zinc-blende and wurtzite-type structures and six in some rock-salt-type compounds. Other rock-salt-type compounds show a different ELI-D topology, i.e. there are 8 (KF, RbF, CaO, SrO), 12 (RbBr, CaTe, SrSe) or 24 (KI, RbI, SrTe) ELI-D valence basins per atom. These variations originate from the almost spherical ELI-D field close to the valence attractors in highly ionic compounds and do not indicate different types of bonding.

Within the precision of ELI-D to recover the formal atomic shell populations all investigated compounds can be described as octet compounds with access electron numbers of the anion E between 7.5 and 8.5, i.e., $\bar{N}_{\text{acc}}^{\text{ELI}}(\text{C}^E) = 8 \pm 0.5$. Due to a large overpopulation of the indium core region is this value in wurtzite-type InN slightly smaller, $\bar{N}_{\text{acc}}^{\text{ELI}}(\text{C}^N) = 7.23$. It is still interpreted as an octet compound because the deviation can be completely attributed to the ELI-D core populations and does not result from an anomaly in the ELI-D valence region.

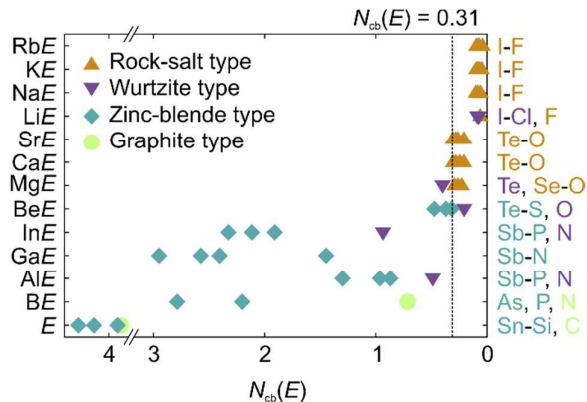


Fig. 6 Optimized stable structures of binary 1:1 compounds and the corresponding numbers of covalent bonds $N_{\text{cb}}^{\text{ELI}}(E)$ for anions.

Within the position-space $8-N$ rule, structure types like the graphite, zinc-blende or wurtzite type should exhibit a high degree of covalent bonding ($N_{\text{cb}}^{\text{ELI}}(E)$ close to 4). On the other hand, compounds of the ionic rock-salt structure should show a low degree of covalent bonding. Figure 6 shows the covalent bond numbers for the anions $N_{\text{cb}}^{\text{ELI}}(E)$. Indeed, the graphite and zinc-blende-type compounds show the highest degrees of covalent bonding and the rock-salt-type compounds show the most ionic bonding patterns. Moreover, there is a clear line that differentiates between these more covalent crystal structures and compounds of the rock-salt type at $N_{\text{cb}}^{\text{ELI}}(E) = 0.31$. Thus, the graphite and zinc-blende type are more stable than the rock-salt type until a very high

degree of ionicity. The wurtzite type occurs with covalent bond numbers between 0.1 and 0.9. Within one row of AE compounds (Figure 6), the wurtzite type plays a kind of mediating role between the covalent zinc-blende and ionic rock-salt type. Below $N_{cb}^{ELI}(E) = 0.31$ wurtzite-type compounds always represent the most ionic compound of a row (InN, AlN, BeO), above $N_{cb}^{ELI}(E) = 0.31$ the wurtzite type occurs only for the most covalent compounds of a row (LiI-LiCl, MgTe).

The presented correlation shows that the position-space representation of the 8-*N* rule is capable to rationalize basic experimental observations. Compared to the method of Mooser and Pearson^[29] and the method of ionic radii^[17,30], the position-space view is *i)* justified by arguments of chemical bonding, *ii)* only relies on one parameter, *iii)* covers a larger range of compounds. The wurtzite type plays the role of a boundary structure type in all three methods although it is structurally very close to the covalent zinc-blende type.

Tab. 1 Estimated parameter ranges of different (pseudo) main-group elements and compound families in the solid state: covalent $CN(E)$ addresses the number of covalently bonded nearest neighbours of the most electronegative component *E*. [*x*; *y*] is an interval including the values of *x* and *y*, [*x*; *y*] includes all values larger or equal to *x* and smaller than *y*.

Bonding	Solid phases	$Q(E)$	$N_{acc}(C^E)$	$N_{val}(E)$	$N_{cb}(E)$	$N_{lp}(E)$	covalent $CN(E)$
not bonded	He, Ne, Ar, Kr, Xe	0	8	8	0	4	0
ionic	Rock-salt type, CsCl type	<0	8	8	0	4	0
polar 2-center	Zintl phases with heteroatomic polyanions e.g. $Ca_3[AlAs_3]$, zinc-blende type, MgAgAs type	<0	8	[4;8]	[4;0]	[0;4]	[4;0], 8
covalent 2-center	Zintl phases	<0	8	[4;8] integer	[4;0] integer	[0;4] integer	[4;0]
covalent 2-center	Diamond-type tetrels, graphite, pnictogens*, chalcogens*, halogens*	0	8	[4;7] integer	[4;1] integer	[0;3] integer	[4;1]
covalent multicenter	B, boron cluster compounds, α -Ga	≤ 0	$\neq 8$	[3;4]	3-center**		>4
covalent multicenter	Alkaline (earth) metals, Al, In, Tl, Pb, Hume-Rothery phases, Laves phases	≤ 0	$\neq 8$	[1;6]	≥ 3 -center**		>4

* Modifications with (pseudo) tetrahedral structure patterns

** For compounds with multicenter bonding, the conceptual meaning of $N_{cb}(E)$ and $N_{lp}(E)$ has to be examined

6. Conclusion & Outlook

The presented position-space representation sets the concept of the 8-*N* rule into a quantum-mechanical framework and describes the case of heteropolar bonding in a consistent and quantitative way. This introduces a new analogy between homopolar and heteropolar bonding situations and shows the connection between the two formal viewpoints on the 8-*N* rule. The decisive point of the formalism presented may be seen in the unification of the formal charges with the very well defined QTAIM effective charge assignment of the pseudo-atomic species. The position-space representation of the 8-*N* rule is capable to rationalize the transition from zinc-blende to rock-salt-type compounds with arguments of chemical bonding.

Table 1 shows the estimated position-space parameter ranges for a variety of different (pseudo) main-group elements and compound families. These ranges represent the expected outcome of possible future investigations and show a first differentiation between the displayed elements and compound families in the context of position-space valence electron counting. The noble gases are chemically non-bonded and have a specific set of parameter values. The MgAgAs-type and Zintl phases with heteroatomic polyanions show a charge transfer and a heteropolar bonding pattern in agreement with the position-space representation of the 8-*N* rule. The rock-salt and CsCl structure types appear in the ionic limit of the concept. Zintl phases with homoatomic bonds within anions and integer numbers of covalent

bonds and lone pairs are polar with respect to the charge transfer between the cations and the anion(s) and fully covalent within the polyanion(s). Concerning their position-space parameter ranges, the rock-salt and CsCl-type compounds as well as the Zintl phases can be included into the group of phases with heteroatomic polyanions, which shows the conceptual overlap between the three groups of compounds. The electronically neutral diamond-type tetrels, graphite and the other element modifications with (pseudo) tetrahedral structure patterns appear in the non-polar 2-center covalent limit of the position-space representation of the 8-*N* rule. The last two rows of Table 1 represent an outlook on (pseudo) main-group elements and compound families with multi-center bonding. Such a bonding situation is characterized by an access electron number different from 8 (see for comparison ELI-D topologies of alkaline (earth) and rare-earth hexaborides^[31] as well as of bcc-Na^[32]). For compounds with multicenter bonding, the conceptual meaning of $N_{cb}(E)$ and $N_{lp}(E)$ has to be examined. A suitable position-space representation of the Wade-Mingos rules has yet to be discovered. The approach using access electron numbers based on ELI-D topologies is independent of the formal octet counting and their interrelation is to be investigated in more detail.

Notes and references

⁵ The approximate equality appears because a QTAIM atom X may also contribute electrons to ELI-D valence regions B_j which do not belong to the access set S_X . However, such contributions are usually very small and can be neglected in most cases.

⁵⁵ The deviations originate from well-known ELI-D characteristics i.e. non-integer core shell populations and the tendency to “overpopulate” lone-pair like regions compared to the formal picture.^[16]

⁵⁵⁵ The position-space analysis yields for InSb: $Q^{\text{eff}}(\text{Sb}) = -0.46$; $\bar{N}_{(\text{In,Sb}B)} = 1.99$; $p_{(\text{In,Sb}B^{\text{Sb}})} = 0.71$; $cc_{(\text{In,Sb}B)} = 0.58$; $\bar{N}_{\text{acc}}^{\text{ELI}}(C^{\text{Sb}}) = 7.97$; $\bar{N}_{\text{val}}^{\text{ELI}}(\text{Sb}) = 5.65$; $N_{\text{cb}}(\text{Sb}) = 2.32$; $\bar{N}(C^{\text{Sb}}) = 45.81$. The position-space analysis yields for GaSe: $Q^{\text{eff}}(\text{Se}) = -0.69$; $\bar{N}_{(\text{Ga,Se}B)} = 1.79$; $p_{(\text{Ga,Se}B^{\text{Se}})} = 0.76$; $cc_{(\text{Ga,Se}B)} = 0.49$; $\bar{N}_{(\text{Ga,Ga}B)} = 2.51$; $\bar{N}_{(\text{Se}B)} = 2.85$; $p_{(\text{Se}B^{\text{Se}})} = 1.00$; $cc_{(\text{Se}B)} = 0.00$; $\bar{N}_{\text{acc}}^{\text{ELI}}(C^{\text{Se}}) = 8.23$; $\bar{N}_{\text{val}}^{\text{ELI}}(\text{Se}) = 6.91$; $N_{\text{cb}}(\text{Sb}) = 1.32$; $\bar{N}(C^{\text{Se}}) = 27.78$.

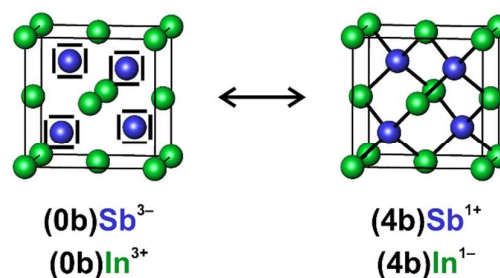
‡ Computational details of the structure optimization: program FHI-aims^[33], PBE functional^[34], 3400 k-points, “safe basis set” defaults.

‡‡ Computational details of the position-space analysis: programs elk2.2.10^[35] and DGrid4.7^[36], PBE functional^[34], 500 k-points; the following elk parameters were adjusted to create artefact-free ELI-D topologies: at least $l_{\text{maxpw}} = 10$, $l_{\text{maxvr}} = 9$, $rgk_{\text{max}} = 10$, $g_{\text{maxvr}} = 20$, basis set defaults.

- R. Ferro, A. Saccone, *Intermetallic Chemistry*, Elsevier, 2008, p. 262 ff.
- Yu. Grin, In: *Comprehensive Inorganic Chemistry II*, vol. 2, Elsevier, 2013, p. 319 ff.
- E. Mooser, W. B. Pearson, *Phys. Rev.*, 1956, **101**, 1608.
- P. Karen, P. McArdle, J. Takats, *Pure Appl. Chem.*, 2014, **86**, 1017.
- E. Zintl, H. Kaiser, *Z. Anorg. Allg. Chem.*, 1933, **211**, 113.
- W. Klemm, E. Bussman, *Z. Anorg. Allg. Chem.*, 1963, **319**, 297.
- H. Schäfer, *Ann. Rev. Mater. Sci.*, 1985, **15**, 1.
- W. B. Pearson, *Acta Crystallogr.*, 1964, **17**, 1.
- A. Kjekshus, *Acta Chem. Scand.*, 1964, **18**, 2379.
- E. Parthé, *Acta Crystallogr.*, 1973, **29**, 2808.
- K. Wade, *Adv. Inorg. Radiochem.*, 1976, **18**, 1.
- D. M. P. Mingos, *Acc. Chem. Res.*, 1984, **17**, 311.
- W. Hume-Rothery, *J. Inst. Met.*, 1926, **35**, 295.
- W. Hume-Rothery, In: *Materials Science and Engineering*, McGraw Hill, 1967.
- U. Mizutani, *Hume-Rothery Rules for Structurally Complex Alloy Phases*, CRC Press, 2011.
- D. Bende, F. R. Wagner, Yu. Grin, *Inorg. Chem.*, 2015, **54**, 3970.
- L. Pauling, *The Nature of the Chemical Bond*, Cornell University Press, 1960.
- R. F. W. Bader, *Atoms in Molecules*, Oxford University Press, 1990.
- a) M. Kohout, *Faraday Discuss.*, 2007, **135**, 43; b) F. R. Wagner, V. Bezugly, M. Kohout, Yu. Grin, *Chem. Eur. J.*, 2007, **13**, 5724; c) F. R. Wagner, M. Kohout, Yu. Grin, *J. Phys. Chem. A*, 2008, **112**, 9814; d) A. Martin Pendas, M. Kohout, M. A. Blanco, E. Francisco, In: *Modern Charge Density Analysis*, Springer, 2012, p. 303 ff.
- a) Yu. Grin, A. Savin, B. Silvi, In: *The Chemical Bond*, Wiley-VCH, 2014, p. 345ff; b) A. D. Becke, K. E. Edgecombe, *J. Chem. Phys.* 1990, **92**, 5397.
- M. Kohout, A. Savin, *Int. J. Quantum Chem.*, 1996, **60**, 875.
- A. I. Baranov, *J. Comput. Chem.*, 2014, **35**, 565.
- S. Raub, G. Jansen, *Theor. Chem. Acc.*, 2001, **106**, 223.
- C. Yeh, Z. W. Lu, S. Froyen, A. Zunger, *Phys. Rev. B*, 1992, **46**, 10086.
- R. Juza, H. Hahn, *Z. Anorg. Allg. Chem.*, 1938, **239**, 282.

- Z. P. Cancarevic, J. C. Schön, M. Jansen, *Chem. Asian J.*, 2008, **3**, 561.
- A. Bach, D. Fischer, M. Jansen, *Z. Anorg. Allg. Chem.*, 2009, **635**, 2406.
- D. Fischer, A. Müller, M. Jansen, *Z. Anorg. Allg. Chem.*, 2004, **630**, 2697.
- E. Mooser, W. B. Pearson, *Acta Crystallogr.*, 1959, **12**, 1015.
- J. K. Burdett, S. L. Price, G. D. Price, *Solid State Commun.*, 1981, **40**, 923.
- C. Börrnert, Yu. Grin, F. R. Wagner, *Z. Anorg. Allg. Chem.*, 2013, **639**, 2013.
- A. I. Baranov, M. Kohout, *J. Comput. Chem.* 2011, **32**, 2064.
- V. Blum, R. Gehrke, F. Hanke, P. Havu, V. Havu, X. Ren, K. Reuter, M. Scheffler, *Comput. Phys. Commun.*, 2009, **180**, 2175.
- J. P. Perdew, K. Burke, M. Ernzerhof, *Phys. Rev. Lett.*, 1996, **77**, 3865.
- Program elk, version 2.2.10, www.elk.sourceforge.net.
- M. Kohout, Program DGrid, version 4.7, Radebeul, 2014.

Table of contents graphic and text:



The 8– N rule in solid-state chemistry is represented by two complementary views. This frontier contribution highlights the new quantum-chemical position-space representation of the 8– N rule which unites the two classical views and shows promising predictive capabilities, in particular for heteropolar bonding situations.